doi:10.1111/j.1558-5646.2010.01214.x

EFFECTS OF GASTEROID FRUITING BODY MORPHOLOGY ON DIVERSIFICATION RATES IN THREE INDEPENDENT CLADES OF FUNGI ESTIMATED USING BINARY STATE SPECIATION AND EXTINCTION ANALYSIS

Andrew W. Wilson,[1,2,3] Manfred Binder,[1,4] and David S. Hibbett[1,5]

[1]*Department of Biology, Clark University, Worcester, Massachusetts 01610*

[2]*E-mail: awilson@chicagobotanic.org*

[4]*E-mail: mbinder@clarku.edu*

[5]*E-mail: dhibbett@clarku.edu*

Received June 28, 2010
Accepted December 4, 2010

Gasteroid fungi include puffballs, stinkhorns, and other forms that produce their spores inside the fruiting body. Gasteroid taxa comprise about 8.4% of the Agaricomycetes (mushroom-forming fungi) and have evolved numerous times from nongasteroid ancestors, such as gilled mushrooms, polypores, and coral fungi, which produce spores on the surface of the fruiting body. Nongasteroid Agaricomycetes have a complex mechanism of forcible spore discharge that is lost in gasteroid lineages, making reversals to nongasteroid forms very unlikely. Our objective was to determine whether gasteromycetation affects the rate of diversification of lineages "trapped" in the gasteroid state. We assembled four datasets (the Sclerodermatineae, Boletales, Phallomycetidae, and Lycoperdaceae), representing unique origins of gasteroid fungi from nongasteroid ancestors and generated phylogenies using BEAST. Using the program Diversitree, we analyzed these phylogenies to estimate character-state-specific rates of speciation and extinction, and rates of transitions between nongasteroid and gasteroid forms. Most optimal models suggest that the net diversification rate of gasteroid forms exceeds that of nongasteroid forms, and that gasteroid forms will eventually come to predominate over nongasteroid forms in the clades in which they have arisen. The low frequency of gasteroid forms in the Agaricomycetes as a whole may reflect the recent origins of many gasteroid lineages.

KEY WORDS: **BiSSE, Diversitree, extinction rates, gasteroid fungi, gasteromycetation, irreversible evolution, puffballs, speciation rates.**

The Agaricomycetes is a diverse group of fungi that produce elaborate reproductive structures such as mushrooms, coral fungi, and puffballs. These fruiting structures can fall within one of two major morphological categories. These are the morphologically diverse nongasteroid forms (e.g., mushrooms, boletes, polypores) and gasteroid forms (i.e., stomach-fungi or puffballs). The Agaricomycetes is largely composed of fungi with a nongasteroid morphology, which is the plesiomorphic condition for the group, whereas gasteroid fungi are sparsely distributed in numerous derived lineages (Thiers 1984; Bruns et al. 1989; Hibbett et al. 1997). Gasteroid fruiting bodies are thought to have evolved as an adaptation to animal dispersal and arid climates (Savile 1955,

[3]Plant Science and Conservation, Chicago Botanic Garden, Glencoe, Illinois, 60022.

1968; Thiers 1984; Bruns et al. 1989). Approximately 8.4% of Agaricomycetes are gasteroid whereas the rest are nongasteroid (Hawksworth et al. 1996).

In nongasteroid Agaricomycetes, spores develop externally on specialized cells called basidia, which grow in the hymenium, the fertile surface of the fungal fruiting body. Nongasteroid spores are launched from the hymenium by a process of forcible spore discharge, known as ballistospory. The mechanism of ballistospory involves rapid energy exchange through the surface tension that is released when two separate formations of liquid, one from the spore and one at the base of the spore, merge. The merging causes the fluid to jump over to the spore, and launches it from the basidium (Buller 1909; Ingold 1971; Turner and Webster 1991; Pringle et al. 2005). This mechanism requires asymmetrical spores with hilar appendages (a minute protuberance at the base of the spore), and curved apical sterigmata (stalks that bear the spores). None of these features are observed in gasteroid Agaricomycetes, which lack ballistospory. The gasteroid fungi also differ from nongasteroid fungi in that the hymenium has become enclosed and has evolved into a structure called the gleba, within which the spores mature. Reversals from gasteroid to nongasteroid forms are highly unlikely, because they would require reevolving a hymenium and the structures responsible for the complex mechanisms involved in ballistospory (Thiers 1984). The hypothesis of the irreversibility of gasteromycetation was tested by Hibbett (2004) in a phylogenetic context. Using a combination of binary- and multistate maximum likelihood analyses, he evaluated the rate of change between five Agaricomycete fruiting morphologies (four nongasteroid and one gasteroid). Models of fruiting body evolution in which the evolution of gasteroid forms is irreversible could not be rejected.

Gasteroid fungi represent a small fraction of the total number of species of Agaricomycetes, but they encompass a tremendous range of morphological diversity (Fig. 1). We focused on three clades that contain diverse gasteroid and nongasteroid taxa. The Sclerodermatineae (Figs. 1A-E) is a suborder within the large, and ecologically important Boletales (Binder and Bresinsky 2002), which includes the nongasteroid genera *Boletinellus, Phlebopus,* and *Gyroporus* and a variety of gasteroid genera such as *Scleroderma* (puffballs), *Astraeus* (earthstar), *Calostoma* (stipitate, gelatinized), and *Pisolithus* (a puffball in which the gleba has been fragmented into individual chambers). The Phallomycetidae (Figs. 1F-J) includes gasteroid genera such as *Geastrum* (earthstar), *Sphaerobolus* ("cannon-ball" fungus, with gleba "packets" that are forcibly ejected from the fruiting body), *Hysterangium* (gelatinized puffball), and *Phallus* (stinkhorn, gelatinized) (Hosaka et al. 2006). The Lycoperdaceae (Figs. 1K-N) is a lineage in the Agaricaceae, with four simple gasteroid genera *Lycoperdon, Bovista, Calvatia,* and *Discisdea* (Larsson and Jeppson 2008). In addition, other morphologically unique gasteroid lineages exist within the Agaricomycetes, such as the Tulostomataceae (stalked puffballs), the Nidulariaceae (birds nest fungi), and simple gasteroid bolete genera *Rhizopogon* and *Melanogaster*, to name a few. Clearly, the gasteroid condition does not preclude morphological diversification, even though gasteromycetation itself is irreversible. Indeed, the range of gasteroid morphologies that are observed in the Agaricomycetes (Fig. 1) suggests that gasteromycetation may offer opportunities to diversify in a new adaptive landscape.

We addressed whether the evolution of the gasteroid morphology affects the rate of diversification in lineages of Agaricomycetes. If gasteromycetation were to reduce diversification rates relative to nongasteroid lineages, then we would expect gasteroid clades to remain small (and therefore be more prone to extinction), compared to their nongasteroid relatives. This expectation is consistent with the current paucity of gasteroid forms across the Agaricomycetes as a whole. On the other hand, if gasteromycetation were to result in an increase in the rate of diversification over nongasteroid forms, then gasteromycetation would be an evolutionary key innovation. More generally, if the gasteroid rate of diversification is positive, but less than that of nongasteroid forms, then we still might expect the number of gasteroid lineages to increase, because transformations to gasteroid forms are irreversible.

To address the diversification consequences of gasteromycetation, we used Binary State Speciation and Extinction analysis (BiSSE; Maddison et al. 2007), which is implemented in Diversitree (FitzJohn et al. 2009). BiSSE estimates character state-specific speciation (μ) and extinction (λ) rates, and rates of transition (q) between binary character states (0 and 1), for a total of six rate parameters (λ_0, λ_1, μ_0, μ_1, q01, and q10). BiSSE allows any of the rate parameters to be constrained to evaluate different hypotheses about character-associated diversification. We focused on gasteromycete diversification in the Sclerodermatineae (Figs. 1A–E), with additional analyses on a more inclusive Boletales dataset, the Phallomycetidae (Figs. 1F-J), and the Lycoperdaceae (Figs. 1K–N). Analysis of multiple independent clades allowed us to assess the generality of results obtained in the Sclerodermatineae, whereas comparison of results from the nested Sclerodermatineae and Boletales datasets addressed the impact of taxon sampling within a single clade.

Materials and Methods

DATASETS

We assembled five datasets representing both gasteroid and nongasteroid morphologies in different taxonomic groups of Agaricomycetes, including two datasets for the Sclerodermatineae with different proportions of gasteroid taxa. We generated original gene sequences to create the Sclerodermatineae datasets, whereas the

Figure 1. Nongasteroid and gasteroid fungal morphologies in the Agaricomycetes. The three rows correspond to the groups Sclerodermatineae (A–E), Phallomycetidae (F-J), and nongasteroid *Chlorophyllum molybdites* (K) with the Lycoperdaceae (L–N). Nongasteroid fungi: A, F, and K. Gasteroid fungi: B–E, G–J, and L–N. (A). *Gyroporus castaneus,* (B) *Astraeus* sp., (C) *Calostoma cinnabarinum,* (D) *Pisolithus tinctorius,* (E) *Scleroderma cepa,* (F) *Gomphus floccosus,* (G) *Trappea darkeri,* (H) *Sphaerobolus stellatus,* (I) *Geastrum floriforme,* (J) *Aseroe rubra,* (K) *Chlorophyllum molybdites,* (L) *Calvatia pachyderma,* (M) *Bovista pila,* (N) *Lycoperdon marginatum.* Photo Credits: A by P.B. Matheny; B–D and N by A.W. Wilson; E–G and K by M. Wood (Mykoweb.com); H, I, L, and M by F. Stevens (Mykoweb.com); J by D.E. Desjardin.

data for the remaining three datasets—the Boletales, the Phallomycetidae, and the Lycoperdaceae—were gathered from previous studies or assembled from sequence data available on GenBank (http://www.ncbi.nlm.nih.gov/GenBank/index.html). We based the taxonomic sampling in each group on current estimates of species richness per genus from the Dictionary of the Fungi (Kirk et al. 2008). This information was used to adjust the numbers of taxa to approach the correct proportions of gasteroid fungi in each clade.

Sclerodermatineae

We extracted DNA from fresh fungal basidiomes and dried herbarium samples. Due to the large amount of pigmentation that is present in Sclerodermatineae species, we attempted a number of DNA extraction methods, including miniprep and maxiprep methods (protocols can be found at http://www.clarku.edu/faculty/dhibbett/protocols.html) and the EZNA Fungal DNA Miniprep kit (Omega Bio-tek, Inc., Doraville, GA). We purified DNA using GeneClean glass milk (Q-BIOgene, www.qbiogene.com).

We used PCR to amplify the nuclear ribosomal 5.8S region with primers ITS1-F (Gardes and Bruns 1993) and ITS4 (White et al. 1990). To amplify the 5′ end of the nrDNA large subunit (25S), we used primers LR0R and LR5 (Vilgalys and Hester 1990). To amplify regions A through C of the protein-coding region ribosomal polymerase two, subunit one (RPB1), we used the published primers RPB1-Af and RPB1-Cr (Matheny et al. 2002), and the newly designed primers RPB1-sA1f (5′-AACT YWACTCGTTTYGCACCCC-3′), and RPB1-sA2r (5′-GCACC CACCTCCCAATTTCTGG-3′). To amplify and sequence ribosomal polymerase two, subunit two (RPB2), regions 5–7, we used various combinations of the published primers RPB2-f5F, RPB2-b7R, RPB2–7R2, RPB2–7.1R, RPB2-a8.0R (Matheny

2005; Binder et al. 2010) along with the newly designed primers RPB2-s5.2F (5′-TGGGGRGACCARAAGAARTC-3′), and RPB2-s7.1R (5′-CTGATTRTGGTC NGGGAAMGG-3′). To amplify and sequence translation elongation factor 1-alpha (ef1α), we used primers EF1–983F, EF1–2218R, EF1–1953R, and EFcf (Rehner and Buckley 2005). PCR and sequencing conditions for the various genes were based on White et al. (1990, for rRNA genes), Matheny et al. (2002, RPB1), Matheny (2005, RPB2), and Rehner and Buckley (2005, ef1α). Primer sequences and maps are available at the Hibbett lab website (http://www.clarku.edu/faculty/dhibbett/Protocols_Folder/Primers/Primers.pdf).

Nearly 40% of the sequences that we generated in this study had to be cloned due to intragenomic heterogeneity or weak amplification. We cloned PCR amplicons using the TA or TOPO TA Cloning Kits (Invitrogen, Carlsbad, CA). We ligated fresh, cleaned, PCR product to pCR 2.1 vectors that were then used to transform MAX efficiency DH5α-T1 chemically competent cells of *Escherichia coli*. We incubated approximately 75 mL of cells in liquid SOC medium at 37°C for up to 24 h on Luria-Bertani (LB) agar prepared with 50 μg/mL of kanamycin and 50 μL of 50 mg/mL of X-gal in dimethylformamide. We screened transformed colonies with PCR using primers M13F and M13R followed by gel electrophoresis (1% agarose) with a 1 kb stepladder. Up to three amplicons of the expected size were chosen for sequencing.

We constructed two datasets for the Sclerodermatineae (Table 1). Sclerodermatineae dataset 1 represents 103 operational taxonomic units (OTUs) and is composed of 214 newly generated sequences (65 25S, 41 5.8S, 37 RPB1, 40 RPB2, 31 ef1α) and 46 sequences acquired from GenBank (38 25S, 2 5.8S, 2 RPB1, 2 RPB2, 2 ef1α). Both nuclear ribosomal DNA and protein-coding sequences are present in 43 OTUs. The remaining 60 OTUs are represented by 25S sequence data only. Sclerodermatineae dataset 2 is a reduced dataset of 76 OTUs where 27 OTUs, represented by 25S sequences, were removed from dataset 1 (Table 1).

Sixty-seven percent of the taxa in Sclerodermatineae dataset 1 are gasteroid (Table 2). This is about equal to the frequency of gasteroid taxa in the clade (68%) based on estimates in the Dictionary of the Fungi (Kirk et al. 2008). Seventy-two percent of the taxa in the Sclerodermatineae dataset 2 are gasteroid, which is slightly higher than the estimates from the Dictionary of the Fungi. Thus, the two Sclerodermatineae datasets represent slightly different proportions of gasteroid forms. It is possible that the Dictionary of the Fungi underestimates the diversity of gasteroid Sclerodermatineae, based on the amount of cryptic diversity that has been detected in the group. Studies of *Astraeus* (Phosri et al. 2007) and *Pisolithus* (Martín et al. 2002) report a surprising number of cryptic taxa in these gasteroid genera. This cryptic diversity is not limited to gasteroid forms as molecular analyses suggest that individual species of *Gyroporus* appear to represent multiple cryptic taxa (A.W.W., unpubl. data). *Chlorogaster dipterocarpi* (Læssøe and Jalink 2004) is a gasteroid species of Sclerodermatineae that was not included in this study because of a lack of sequence data.

Boletales

We used the dataset from Binder and Hibbett (2006), which consists of 485 nuclear ribosomal 25S sequences. This dataset contains approximately 15% gasteroid taxa, which is less than the 25% estimated using the Dictionary of the Fungi (Table 2). The Boletales dataset includes 31 species (6.4%) of Sclerodermatineae, with 402 species representing all of the other major clades of Boletales; the remaining 52 species represent outgroup taxa. 72 species (14.8%) in the Boletales dataset are gasteroid, including 19 species of Sclerodermatineae, with the remainder distributed among the Suillineae (32 species), Boletineae (15 species), Serpulaceae (three species), and the outgroup taxa (three species).

Phallomycetidae

For analyses of the Phallomycetidae, we modified the dataset of Hosaka et al. (2006), which consists of nrLSU, mtSSU, atp6, RPB2, EF1α sequence data for 213 taxa. For this study, we removed 89 taxa representing the gasteroid morphology from the original Hosaka et al. (2006) dataset, which brought the dataset to 52% gasteroid fungi, and making it slightly greater than the estimated 43.5% gasteroid fungi in the Phallomycetidae (Table 2).

Lycoperdaceae

This dataset comprises 25S sequences from GenBank and is largely based on the Lycoperdaceae sensu Larsson and Jeppson (2008). We included additional 25S sequences for nongasteroid closely related to the Lycoperdaceae. The Lycoperdaceae dataset is approximately 50% gasteroid, which is greater than the 32% estimated using the Dictionary of the Fungi (Table 2).

PHYLOGENETIC ANALYSES

We generated ultrametric trees for each dataset using BEAST version 1.4.6 (Drummond and Rambaut 2007). We used BEAUTi version 1.4.6 to create XML files with the following analytical settings: GTR model, uncorrelated relaxed clock with lognormal rate distribution; Tree Prior set to Yule Process speciation; running 10 million generations, sampling every 1000th tree. For the Boletales dataset, we removed the operators subtreeSlide, narrowExchange, wideExchange, and wilsonBalding from the XML file to estimate branch lengths without branch swapping. By removing these functions, BEAST will only make adjustments to the branch lengths and not the topology of the starting tree, which was supplied by the Binder and Hibbett (2006) study. As a result, we were able to limit the computational difficulty in analyzing such a

Table 1. Taxa sampled and GenBank accession numbers for Sclerodermatineae dataset.

Genus	Species	ID	Location	Dataset 1	Dataset 2	5.8S	25S	RPB1	RPB2	ef1α
Astraeus	hygrometricus	MB 05–029	Massachusetts USA	x	x	**EU718087**	**DQ682996**	**FJ536586**	**FJ536623**	**FJ536663**
	hygrometricus	MEL2238785		x	x		**EU718157**			
	hygrometricus	PDD88503		x	x		**EU718158**			
	pteridis	Ashy 3	Switzerland	x	x	**EU718088**	AF336238	**FJ536587**	**FJ536624**	**FJ536664**
	asiaticus	Arora 02–121	Thailand	x	x	**EU718089**	DQ644199	**FJ536588**	**FJ536625**	**FJ536665**
	sp.	Arora 00–17		x	x		DQ517425			
Boletinellus	merulioides	MB 02–199	Massachusetts USA	x	x	DQ200922	AY684153	DQ435803	DQ366281	DQ056287
	rompelii	No 1192		x	x		**EU718159**			
Calostoma	berkeleyii	AWW268	Malaysia	x	x	**EU718090**	**EU718128**	**FJ536589**	**FJ536626**	**FJ536666**
	berkeleyi	JFK77	Malaysia	x			**FJ710204**			
	cinnabarinum	AWW136	Massachusetts USA	x	x	AY854064	AY645054	AY780939	AY857979	AY879117
	aff. cinnabarinum	F1120877	China	x			**EU718160**			
	fuscum	OKM 23918	Western Australia	x	x	**EU718091**	**EU718129**	**FJ536590**	**FJ536627**	
	fuscum	PDD70777		x	x		**EU718161**			
	insignis	Arora 98–31	Thailand	x	x	**EU718092**	**EU718130**		**FJ536628**	
	japonicum	TKG-SC-40701	Japan	x	x	**EU718093**	**EU718131**	**FJ536591**	**FJ536629**	
	japonicum	OKM22412		x			**EU718162**			
	junghuhnii	VC 1151		x	x		**EU718163**			
	lutescens	1329		x	x		**EU718164**			
	orirubra	HKAS32119		x	x		**EU718165**			
	ravenellii	510	North Carolina USA	x	x	**EU718094**	**EU718132**	**FJ536592**	**FJ536630**	**FJ536667**
	ravenellii	462		x			EU718166			
	rodwayi	GMM 7572	New Zealand	x	x	**EU718095**	**EU718133**		**FJ536631**	
	rodwayii	PDD69216		x	x		**FJ600321**			
	rodwayii	PDD71749		x			**FJ710205**			
	sarasinii	DED7660	Malaysia	x	x	**EU718096**	**EU718134**	**FJ536593**	**FJ536632**	**FJ536668**
	sarasinii	AWW244		x			**FJ710206**			
	sp.	HKAS38133	China	x	x	**EU718097**	**EU718135**		**FJ536633**	
	sp.	HKAS38139	China	x	x	**EU718098**	**EU718136**	**FJ536594**	**FJ536634**	
	sp.	PDD71264b		x						
Diplocystis	wrightii	Ang1		x	x		DQ644134			
	wrightii	DH2002		x			DQ534665			
	wrightii	PR4718		x			DQ644135			
Gyrodon	merulioides	22/98		x	x		AF336239			
	merulioides	NCJ12		x	x		AY612807			

Continued.

Table 1. Continued.

Genus	Species	ID	Location	Dataset 1	Dataset 2	5.8S	25S	RPB1	RPB2	ef1α
Gyroporus	castanaeus	Gc1	Germany	x	x	**EU718099**	AF336252	**FJ536595**	**FJ536635**	**FJ536669**
	castanaeus	239–97	USA	x	x	**EU718100**	AF336253	**FJ536596**	**FJ536636**	**FJ536670**
	castanaeus	REH8804	Thailand	x	x	**EU718101**	**EU718137**	**FJ536597**	**FJ536637**	**FJ536671**
	castanaeus	Arora01 512		x			**FJ710209**			
	castaneus	F1086418		x			**EU718167**			
	castaneus	Gc2		x			**EU718168**			
	aff. austrocastaneus	E4600		x			**EU718169**			
	aff. austrocastaneus	E4879c		x			**FJ710208**			
	aff. austrocastaneus	E843c		x			**EU718170**			
	cyanescens	MB 05–001	USA	x	x	**EU718102**	**EU718138**	**FJ536598**	**FJ536638**	**FJ536672**
	cyanescens	Gcy2		x			AF336254			
	cyanescens	REH8819		x			**EU718172**			
	aff. cyanescens	REH8821	Western Australia	x	x	**EU718103**	**EU718139**	**FJ536599**	**FJ536639**	**FJ536673**
	aff. cyanescens	E8758c		x			**EU718171**			
	aff. cyanescens	E486		x			**EU718173**			
	aff. cyanescens	E5685		x			**EU718174**			
	pseudocyanescens	OKM23719	Western Australia	x	x	**EU718104**	**EU718140**	**FJ536600**	**FJ536640**	
	purpurinus	Leacock 3737	Illinois, USA	x	x	**EU718105**	**EU718141**	**FJ536601**	**FJ536641**	**FJ536674**
	sp.	REH8799	Thailand	x	x	**EU718106**	**EU718142**	**FJ536602**	**FJ536642**	**FJ536675**
	sp.	Arora 00–429	Zimbabwe	x	x	**EU718107**	**EU718143**	**FJ536603**	**FJ536643**	**FJ536676**
	sp.	E8155		x			**EF561627**			
	sp.	REH8805		x			**EU718175**			
	subalbellus	OKM25477	Texas, USA	x	x	**EU718108**	**EU718144**	**FJ536604**	**FJ536644**	**FJ536677**
Phlebopus	beniensis	Omon 98.015		x	x		AY612822			
	marginatus	REH8883	Eastern Australia	x	x	**EU718109**	**EU718145**	**FJ536605**	**FJ536645**	**FJ536678**
	marginatus	MEL2145841		x	x		**FJ600322**			
	portentosus	php1		x	x	**EU718110**	AF336260	**FJ536606**	**FJ536646**	**FJ536679**
	sudanicus	CBS481.89		x	x		AF336261			
	sp.	REH8795	Thailand	x	x	**EU718111**	**FJ153623**	**FJ536607**	**FJ536647**	**FJ536680**
Phaeogyroporus	sp.	OKM23801		x	x		AY612816			
Pisolithus	albus	PERTH. . .4683		x	x		**EU718176**			
	albus	OSC27549		x	x		DQ682997			
	arhizus	588		x	x		AF336262			
	aurantioscabrosus	AWW297	Malaysia	x	x	**EU718112**	**EU718146**	**FJ536608**	**FJ536648**	**FJ536681**
	sp.	ECV3205	California USA	x	x	**EU718113**	**EU718147**	**FJ536609**	**FJ536649**	
	sp.	PERTH. . .4888		x	x		**EU718177**			
	tinctorius	AWW219	Massachusetts USA	x	x	**EU718114**	**EU718148**	**FJ536610**	**FJ536650**	**FJ536682**

Continued.

Table 1. Continued.

Genus	Species	ID	Location	Dataset 1	Dataset 2	5.8S	25S	RPB1	RPB2	ef1α
Scleroderma	areolatum	AWW211	Massachusetts USA	x	x	**EU718115**	**EU718149**	**FJ536611**	**FJ536651**	**FJ536683**
	areolatum	PBM2208	W. Australia	x	x	**EU718116**	**EU718150**	**FJ536612**	**FJ536652**	**FJ536684**
	areolatum	Sar1		x	x		AF336263			
	bovista (laeve)	MCA242	North Carolina USA	x	x	**EU718117**	DQ677138	**FJ536613**	**FJ536653**	**FJ536685**
	bovista	W#1149		x	x		AF336264			
	bermudense	BZ3961	Belize	x	x	**EU718118**	DQ644137	**FJ536614**	**FJ536654**	**FJ536686**
	cepa	184		x	x		AF336265			
	citrinum	AWW212	Massachusetts USA	x	x	**EU718119**	**EU718151**	**FJ536615**	**FJ536655**	**FJ536687**
	citrinum	SC1		x	x		AF336266			
	columnare	JMCR77		x	x		AF261533			
	dictyospora			x	x		AF336267			
	echinatum	MS34		x	x		AF336268			
	fuscum	Trappe26575		x	x		**EU718178**			
	laeve	OSC27936		x	x	**EU718120**	DQ683003	**FJ536616**		
	meridionale	AWW218	Massachusetts USA	x	x	**EU718121**	**EU718152**	**FJ536617**	**FJ536656**	**FJ536688**
	mcalpinei	OSC 24605		x	x	**EU718122**	DQ682999		**FJ536657**	
	polyrhizum	AWW216	Massachusetts USA	x	x	**EU718123**	**EU718153**	**FJ536618**	**FJ536658**	**FJ536689**
	polyrhizum	594		x	x		DQ683000			
	verrucosum			x	x		AF336271			
	sinnamariensis	AWW254	Malaysia	x	x	**EU718124**	**EU718154**	**FJ536619**	**FJ536659**	**FJ536690**
	sinnamariensis			x			AF071531			
	sp. White	AWW260	Malaysia	x	x	**EU718125**	**EU718155**	**FJ536620**	**FJ536660**	**FJ536691**
	sp. Brown	AWW311	Malaysia	x	x	**EU718126**	**EU718156**	**FJ536621**	**FJ536661**	**FJ536692**
	sp.			x	x		DQ644136			
	sp.	Arora 99–17		x	x		**EU718179**			
	sp.	MCA2168		x	x		**EU718180**			
	sp.	MEL2295738		x			**EU718181**			
	sp.	HKAS43607		x			**FJ710210**			
Tremellogaster	surinamensis	MCA 1985	Guyana	x	x	**EU718127**	DQ534664	**FJ536622**	**FJ536662**	**FJ536693**
Veligaster	columnaris			x			AF336273			
	columnaris			x			DQ683002			

Original sequence created for this study appear in bold.

Table 2. Frequencies of gasteroid and nongasteroid forms in Sclerodermatineae, Boletales, Phallomycetidae, and Lycoperdaceae, based on sampled diversity (dataset), estimated diversity from Dictionary of the Fungi (DoF), and predicted equilibrium frequencies from BiSSE parameters under a model of no reversals (EQ freq).

	Gasteroid frequencies					Non-gasteroid frequencies		
	No. of Taxa	Gasteroid origins	Dataset	DoF	EQ $freq_1$	Dataset	DoF	EQ $freq_0$
Sclerodermatineae								
Dataset 1	103	2	67.0%	67.6%	100.0%	33.0%	32.4%	0.0%
Dataset 2	76	2	72.4%		100.0%	27.6%		0.0%
Boletales	485	21	15.2%	24.6%	100.0%	84.8%	75.4%	0.0%
Phallomycetidae	124	3	52.4%	43.5%	100.0%	47.6%	56.5%	0.0%
Lycoperdaceae	112	1	50.9%	32.1%	100.0%	49.1%	67.9%	0.0%

large dataset by removing the complications of branch swapping. We used neighbor-joining analyses with maximum likelihood distances to generate starting trees for all datasets with the exception of the Boletales dataset which used the Bayesian consensus tree from Binder and Hibbett (2006) for the starting tree.

For each dataset in this study, we ran three separate BEAST analyses resulting in three tree files each containing 10,000 trees. For each tree file, we empirically estimated the trees to be removed as the burnin trees using Tracer version 1.4 (Drummond and Rambaut 2007) to identify the point at which trees reached a stable plateau of posterior likelihood values. We used LogCombiner version 1.4.6 (Drummond and Rambaut 2007) to remove the burnin trees and to combine all posterior trees from each of the three BEAST tree files. Using LogCombiner version 1.4.6, we resampled the combined posterior tree file to make a "BiSSE tree file" of 50 trees for analysis in BiSSE. We generated consensus trees for each of the BiSSE tree files using TreeAnnotator version 1.4.6 (Drummond and Rambaut 2007). Using these consensus trees, we determined the number of origins of the gasteromycete morphology assuming irreversibility under parsimony using MacClade version 4.07 (Maddison and Maddison 2005).

DIVERSIFICATION ANALYSES

We used BiSSE (Maddison et al. 2007) to estimate the rate of speciation (λ) and extinction (μ) and state transformations (q01 and q10) associated with nongasteroid (state 0) and gasteroid (state 1) fruiting body forms. BiSSE analyses were implemented in Diversitree version 0.4–3 (FitzJohn et al. 2009), a package developed for the statistical application R (http://www.r-project.org/). We estimated parameters of unconstrained/"reversible" models, in which transformation rates between gasteroid and nongasteroid forms were unconstrained (i.e., q01 and q10 were allowed to take any value), and constrained/"irreversible" models, in which the rate of transformations from gasteroid to nongasteroid forms (q10) was restricted to 0 (q01 was unconstrained). Because these models are not nested, we used a difference of two units in log likelihood scores as a criterion for "strong" support of one model over another (Pagel 1999). The purpose of these comparisons was to assess whether we could reject our a priori assumption that the loss of gasteromycetation is irreversible.

Preliminary analyses using the Mesquite implementation of BiSSE (Maddison et al. 2007) generated unexpected results, in which the constrained models had superior likelihood scores compared to unconstrained models. These results (not shown) suggested that the parameter optimization elements of the Mesquite implementation of BiSSE are challenged by our datasets to find globally optimal parameter values. Therefore, we employed a two-step process using Markov chain Monte Carlo (MCMC) sampling followed by maximum likelihood (ML) optimization, which is intended to more effectively search model space for optimal parameters. In the MCMC step, we sampled rate parameters on each of the 50 trees from each BiSSE tree file. Each MCMC iteration samples a set of rate parameters and records the likelihood score for the model. We analyzed each Sclerodermatineae dataset with 10,000 iterations per tree. The same approach was used for the larger Boletales, Phallomycetidae and Lycoperdaceae datasets, except that we only performed 1000 iterations per tree. We removed the first one-fourth of the states sampled from each model/dataset/tree as part of the burnin and calculated the means and the 95% posterior densities for distributions of state-associated speciation and extinction parameters from the remaining states. In the second step of the analysis, we attempted to obtain optimal models, using the best models sampled during each of the 50 MCMC analyses as starting points for ML optimization. We then calculated the mean parameter values and likelihoods, and compared models using the Akaike information criterion (AIC). The likelihood scores given by Diversitree are proportional to the likelihood values (they are not negative log likelihoods, as are typically reported) but they can be used to calculate AIC scores so analyses of different models on the same dataset can be compared (R. Fitzjohn, pers. comm.).

The mean values for ML parameters were used to calculate the relative diversification rate (r_{rel}) between nongasteroid and

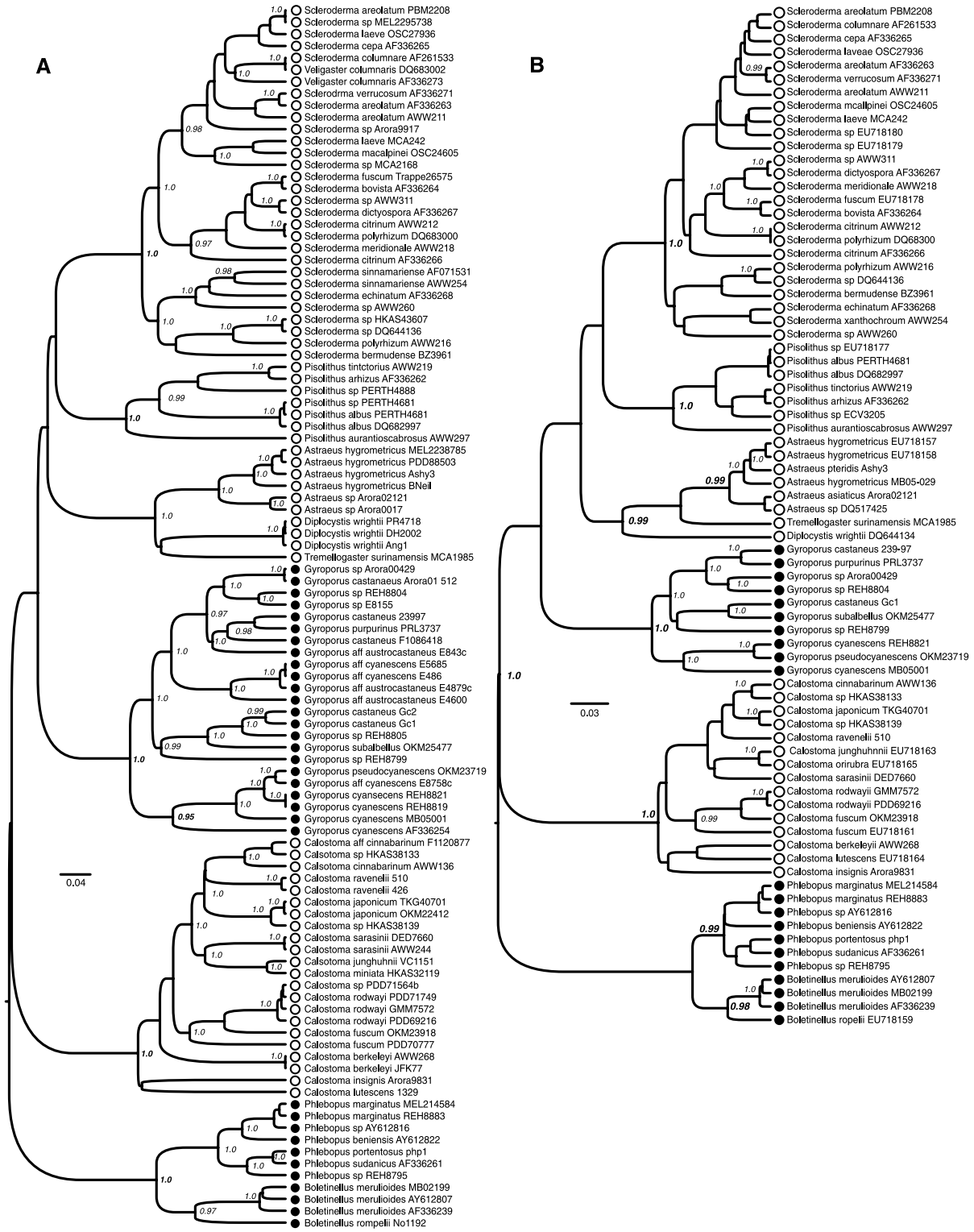

Figure 2. Sclerodermatineae consensus trees of 50 posterior BEAST trees. (A) Sclerodermatineae dataset 1. (B) Sclerodermatineae dataset 2. Closed circles represent nongasteroid forms whereas open circles represent gasteroid forms. Numbers indicate nodes with ≥0.99 posterior probability.

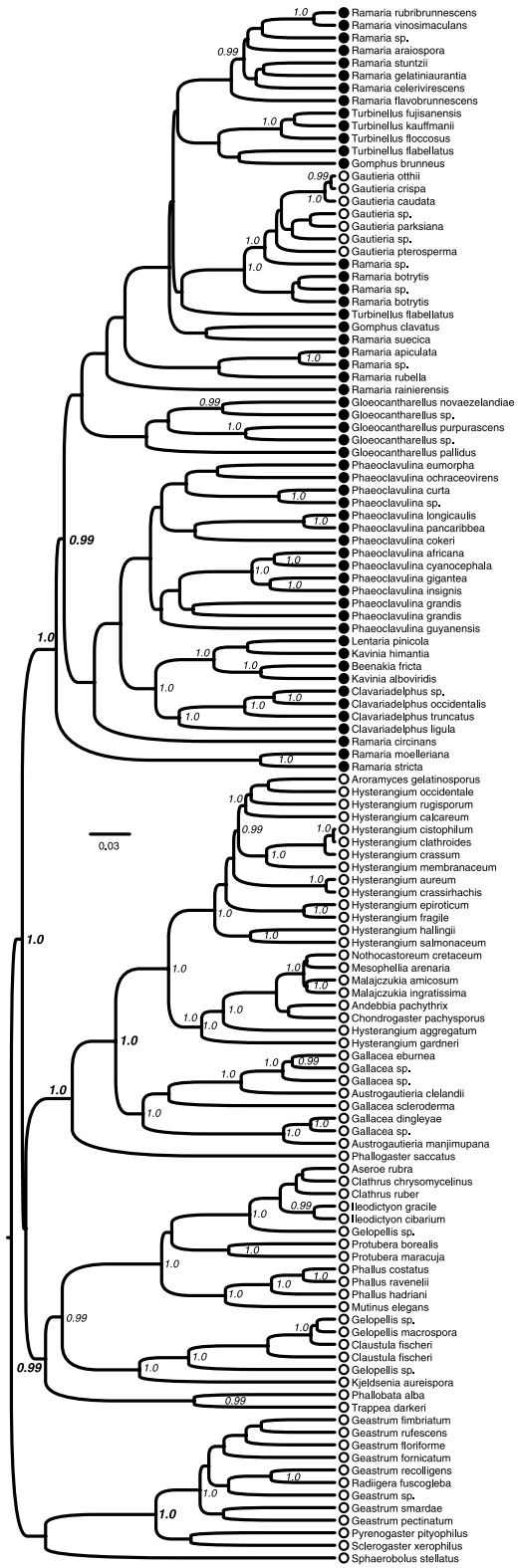

Figure 3. Phallomycetidae consensus tree of 50 posterior BEAST trees. Closed circles represent nongasteroid forms whereas open circles represent gasteroid forms. Numbers indicate nodes with ≥0.99 posterior probability.

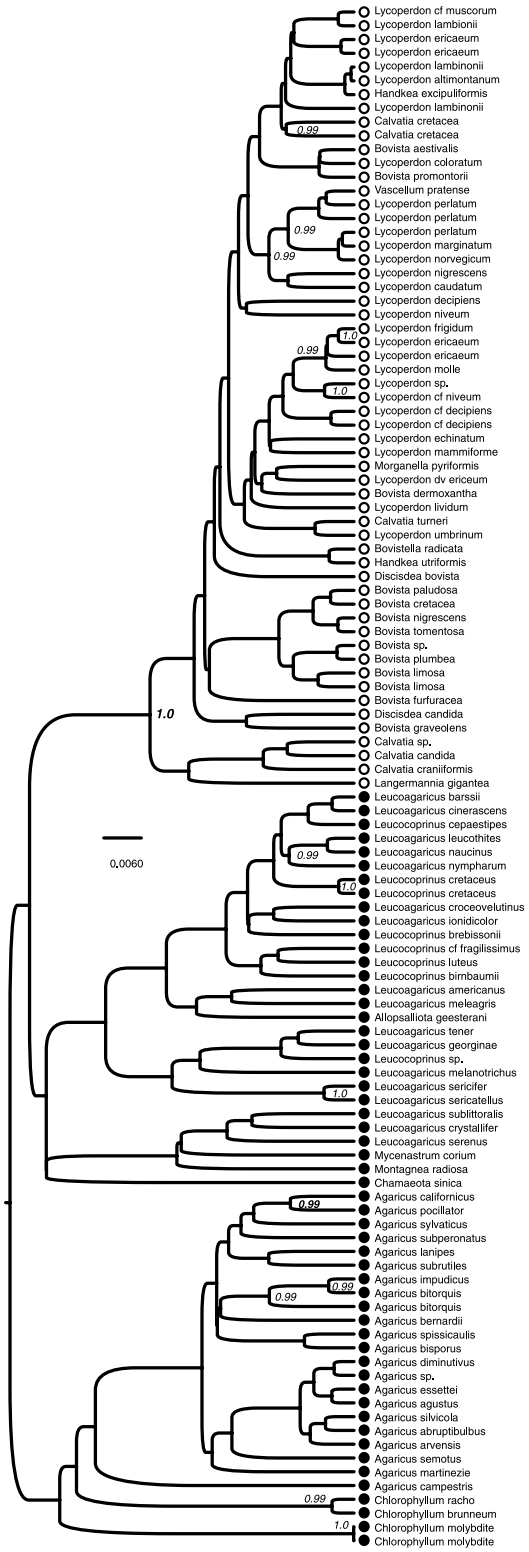

Figure 4. Lycoperdaceae consensus tree of 50 posterior BEAST trees. Closed circles represent nongasteroid forms whereas open circles represent gasteroid forms. Numbers indicate nodes with ≥0.99 posterior probability.

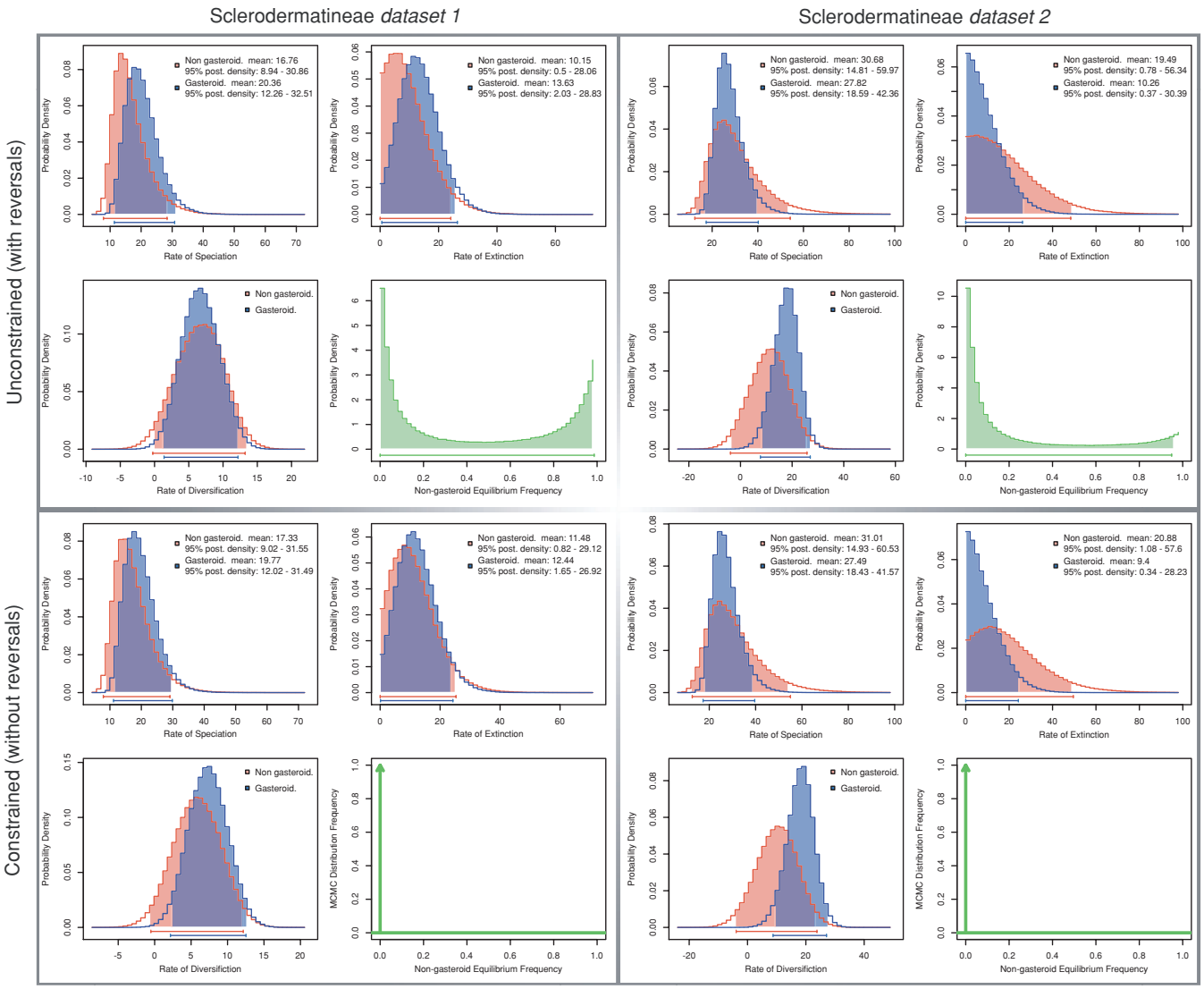

Figure 5. Histograms of speciation, extinction, and diversification parameters for nongasteroid and gasteroid character states and equilibrium frequencies estimated from BiSSE MCMC analyses. Analyses under unconstrained (with reversals) and constrained (without reversals) models (rows) were performed on Sclerodermatineae datasets 1 and 2 (columns). Parameter 95% highest posterior densities for character states indicated by colored shading and horizontal bars below histogram.

gasteroid fruiting forms. This was calculated as the rate of diversification of nongasteroid lineages ($\lambda 0 - \mu 0 = r0$) divided by the rate of diversification of gasteroid lineages ($\lambda 1 - \mu 1 = r1$) (or $r0/r1 = r_{\mathrm{rel}}$). A relative diversification rate greater than one would indicate that gasteroid forms have a lower rate of diversification than nongasteroid forms. Equilibrium state frequencies of gasteroid and nongasteroid forms were calculated according to equation (13) of Maddison et al. (2007). These frequencies were used to determine the potential effect of the estimated parameter rates on the composition of gasteroid and nongasteroid fungi in the Agaricomycetes, but these frequencies assume that the rates will remain constant over evolutionary time. The equilibrium frequency calculation was done using Diversitree's "diversitree:::bisse.stationary.freq" function.

Results

MOLECULAR DATA

The minimum and maximum length for sequences generated for the Sclerodermatineae datasets are described in online Supporting Information Table S1, along with intron lengths and identities (Hopple and Vilgalys 1999; Matheny et al. 2002, 2007). Sclerodermatineae dataset 1 is 4953 characters in length with a total of 2109 parsimony informative characters. Dataset 2 is 4948 characters long with 2073 parsimony informative characters.

Lengths for the other datasets used in this study are: 1071 characters for the Boletales (523 parsimony informative), 3543 characters for the Phallomycetidae (1533 parsimony informative), 775 characters for the Lycoperdaceae (118 parsimony

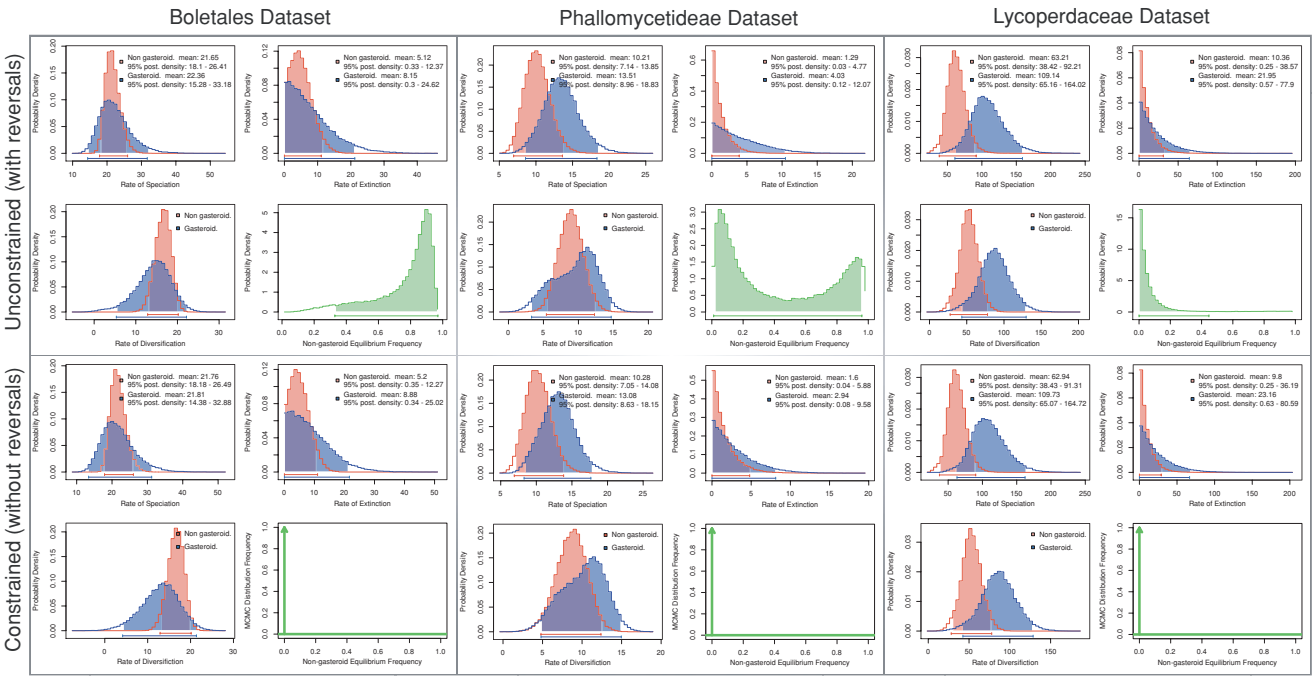

Figure 6. Histograms of speciation, extinction, and diversification parameters for nongasteroid and gasteroid character states and equilibrium frequencies estimated from BiSSE MCMC analyses. Analyses under unconstrained (with reversals) and constrained (without reversals) models (rows) were performed on Boletales, Phallomycetidae, and Lycoperdaceae datasets (columns). Parameter 95% highest posterior densities for character states indicated by colored shading and horizontal bars below histogram.

informative). Lists of included sequences and information on the taxonomic composition of each dataset can be found in online Supporting Information Tables S2a–c and S3a–d, respectively.

PHYLOGENETIC ANALYSES

The Sclerodermatineae (Fig. 2) phylogenetic trees are consistent with results of previous analyses by Binder and Bresinsky (2002) and separate analyses by A.W.W. (unpubl. data). The taxonomic significance of these results will be addressed elsewhere. Similarly, the topologies for the Boletales (not shown), Phallomycetidae (Fig. 3), and Lycoperdaceae (Fig. 4) are largely consistent with previous analyses in these groups (Binder and Hibbett 2006; Hosaka et al. 2006; Larsson and Jeppson 2008). The tree lengths calculated under parsimony suggest that anywhere from one (Lycoperdaceae) to 21 (Boletales) independent origins of the gasteroid morphology have occurred in the groups analyzed in this study (Table 2).

DIVERSIFICATION ANALYSES

The 95% highest posterior density distributions for state-specific speciation and extinction rates estimated with MCMC were largely overlapping in every dataset, with either the unconstrained (reversible) or constrained (irreversible) models of fruiting body evolution (Figs. 5 and 6). Following the MCMC analyses, optimal unconstrained and constrained models were estimated on each of the five datasets, using the best models obtained in each of 50 MCMC searches as starting points for likelihood optimizations. In the optimizations, likelihoods of unconstrained models were greater than those of constrained models, except in the Sclerodermatineae dataset 2 and Lycoperdaceae datasets, in which the constrained models had a slightly higher average likelihood than the unconstrained models (Tables 3 and 4). Six of the searches converged on similar optimal models, with modest variance in model parameters (Figs. 7 and 8, Table 4). However, four other searches (estimating unconstrained models for Sclerodermatineae datasets 1 and 2 and both constrained and unconstrained models for the Lycoperdaceae dataset) returned a set of models with high variance in parameter estimates (Figs. 7 and 8). AIC scores suggested that the constrained models are preferred for three datasets (Sclerodermatineae datasets 1 and 2 and Lycoperdaceae), whereas the unconstrained models are preferred for the Boletales and Phallomycetidae datasets (Tables 3 and 4). Two models were rejected ($\Delta \log L > 2$), including the constrained models for the Boletales and Phallomycetidae datasets. Thus, a total of 10 models were generated in ML optimization, of which eight could not be rejected (Tables 3 and 4). Net diversification rates of gasteroid forms were higher than those of nongasteroid forms in all but one of the nonrejected models (Tables 3 and 4). Six of the nonrejected models predict that gasteroid forms will be more common than nongasteroid forms at equilibrium, including three of the unconstrained models, which suggested that the equilibrium frequencies of gasteroid forms will range from 85% to 100% (Tables 3 and 4).

Table 3. Means for BiSSE state-associated diversification parameters and related statistics under an unconstrained model and a model assuming irreversibility (q10=0). Values reported are means of 50 optimizations from maximum likelihood analyses. Parameter variances are in parentheses.

Model constraint	Rate parameters	Sclerodermatineae dataset 1	Sclerodermatineae dataset 2
None	λ_0	12.89(5.05)	24.10(22.47)
	λ_1	19.15(3.90)	23.16(4.03)
	μ_0	4.67(17.61)	11.79(74.90)
	μ_1	12.66(10.00)	2.91(14.02)
	q01	9.18E-2(2.30×10^{-02})	0.78(0.39)
	q10	0.16(1.26×10^{-02})	0.24(0.10)
	r_0	8.23	12.32
	r_1	6.49	20.25
	r_{rel}	1.27	0.61
	AIC	−259.04	−270.73
	log L	135.5206	141.3645
	EQ $freq_0$	0.95	0
q10=0	λ_0	15.23(3.2×10^{-06})	24.50(3.01)
	λ_1	14.73(3.11×10^{-06})	21.83(0.41)
	μ_0	8.19(5.99×10^{-06})	15.43(3.35)
	μ_1	5.93(6.88×10^{-06})	0.67(7.37×10^{-02})
	q01	0.63(2.04×10^{-08})	1.00(2.52×10^{-03})
	r_0	7.04	9.07
	r_1	8.80	21.17
	r_{rel}	0.80	0.43
	AIC	**−260.50**	**−274.22**
	log L	135.2490	142.1106
	Δlog L	0.2716	−0.7
	EQ $freq_0$	0	0

Bold values indicate the model supported by Akaike's information criterion.

Discussion

We used BiSSE, implemented in Diversitree, to estimate diversification rates of nongasteroid and gasteroid lineages in four clades of Agaricomycetes (two of which, the Boletales and Sclerodermatineae, are nested), with and without assuming irreversibility of the gasteroid condition. We used a two-step approach, utilizing MCMC sampling followed by ML optimization to search parameter space. Results of some ML searches (including the surprising finding that some constrained analyses produced models with likelihoods that were superior to those of competing unconstrained models) suggest that our analyses may not have discovered globally optimal models. Nonetheless, many aspects of our results are consistent across clades and analyses, and suggest that there are general evolutionary tendencies of gasteroid versus nongasteroid lineages.

None of the MCMC analyses suggested that there is a significant difference in speciation or extinction rates between gasteroid and nongasteroid lineages (Figs. 5 and 6). However, seven of the eight nonrejected ML models suggest that gasteroid forms have a higher net diversification rate than nongasteroid forms, and six of the nonrejected models suggest that gasteroid forms will come to predominate at equilibrium. These conclusions do not depend on an assumption of irreversibility of the gasteroid condition; all but one of the unconstrained models suggest that gasteroid forms diversify faster than nongasteroid forms, and three of these models suggest that gasteroid forms will come to represent 85–100% of the diversity in their clades at equilibrium. One model, the unconstrained model for Sclerodermatineae dataset 1, suggested that gasteroid forms represent evolutionary dead-ends that may be headed for extinction (the predicted equilibrium frequency of gasteroid forms is only 5%). However, the competing model assuming irreversible evolution of gasteroid forms could not be rejected (in fact, it is slightly superior according to the AIC).

Models suggesting irreversibility of gasteroid forms were rejected in two datasets, the Boletales and Phallomycetidae. Even in these cases, the unconstrained models suggest that gasteroid forms will comprise 37–85% of the diversity at equilibrium. In sum, we conclude that gasteromycetes are evolutionarily "successful"

Table 4. Means for BiSSE state-associated diversification parameters and related statistics under an unconstrained model and a model assuming irreversibility (q10=0). Values reported are means of 50 optimizations from maximum likelihood analyses. Parameter variances are in parentheses.

Model constraint	Rate parameters	Boletales	Phallomycetidae	Lycoperdaceae
None	λ_0	21.23(6.03×10^{-02})	9.49(0.80)	57.70(84.80)
	λ_1	21.19(0.47)	12.27(1.01)	98.54(290.46)
	μ_0	4.70(0.26)	6.09×10^{-03} (2.78×10^{-04})	1.28(1.70)
	μ_1	3.00(0.59)	1.77(4.90)	3.96(20.05)
	q01	0.64(1.65×10^{-04})	0.26(2.94×10^{-03})	1.19(0.11)
	q10	2.11(1.40×10^{-02})	0.19(1.25×10^{-03})	1.75×10^{-02} (1.39×10^{-03})
	r_0	16.26	9.49	56.36
	r_1	18.19	10.50	94.58
	r_{rel}	0.91	0.90	0.60
	AIC	**−1701.66**	**−305.98**	−747.43
	log L	856.83	158.99	379.7155
	EQ $freq_0$	0.63	0.15	4.43×10^{-04}
q10=0	λ_0	21.21(0.21)	10.45(7.82×10^{-08})	57.54(59.35)
	λ_1	20.75(2.35)	12.23(6.35×10^{-02})	92.80(228.04)
	μ_0	4.39(0.71)	0	0.25(0.51)
	μ_1	4.53(2.85)	0	1.42(10.33)
	q01	0.92(1.72×10^{-03})	0.66(1.30×10^{-09})	1.30(6.62×10^{-02})
	r_0	16.82	10.45	57.29
	r_1	16.23	12.23	91.38
	r_{rel}	1.04	0.85	0.63
	AIC	−1688.28	−302.49	**−749.92**
	log L	849.14	156.2463	379.9620
	Δlog L	7.69	2.74	−0.2465
	EQ $freq_0$	0	0	0

Bold values indicate the model supported by Akaike's information criterion.

forms that, assuming the relative diversification rates between states remain constant, may eventually become dominant in most of the clades in which they have arisen.

In almost all of our analyses, the predicted equilibrium frequencies of gasteroid forms exceed the described proportions of gasteroid forms based on current taxonomy (the unconstrained Sclerodermatineae 1 analysis being the only exception) (Table 2). Taken at face value, the discrepancies between predicted and observed equilibrium frequencies imply that these clades have not yet reached equilibrium. Alternatively, errors in estimates of model parameters obtained with BiSSE could result in errors in equilibrium predictions. Our analysis does not permit us to assess the accuracy of rate parameter estimates from BiSSE. The program performed well in prior simulations, although μ was difficult to estimate (Maddison et al. 2007), and some aspects of our results suggest that our datasets provide difficult ML optimization challenges.

The two Sclerodermatineae datasets contain 103 and 76 species, with 67–72% gasteroid taxa, which compares well with the documented diversity of the clade (Kirk et al. 2008), which has 74 described species, including 68% gasteroid taxa (online Supporting Information Table S3). The remaining three datasets, Boletales, Phallomycetidae, and Lycoperdaceae, contain between 23% (Lycoperdaceae) and 38% (Boletales) of the known diversity in each group. Sampling in these datasets was adjusted to approximate the actual proportions of the genera in each of the focal clades, based on the numbers of described species in each group (Kirk et al. 2008). Nonetheless, taxon sampling is a potential source of error in our analyses; none of our datasets includes all of the known species in the focal clade, and the proportions of gasteroid taxa sampled are not identical to the proportions of gasteroid taxa that have been described. Moreover, the actual diversity in each of the focal clades is not known, and, based on diversity estimates for fungi as a whole (Hawksworth 1991), the described diversity may underestimate the actual diversity in each group. Nevertheless, the relative diversification rates and predicted equilibrium frequencies are largely consistent across datasets, suggesting that our general conclusions about

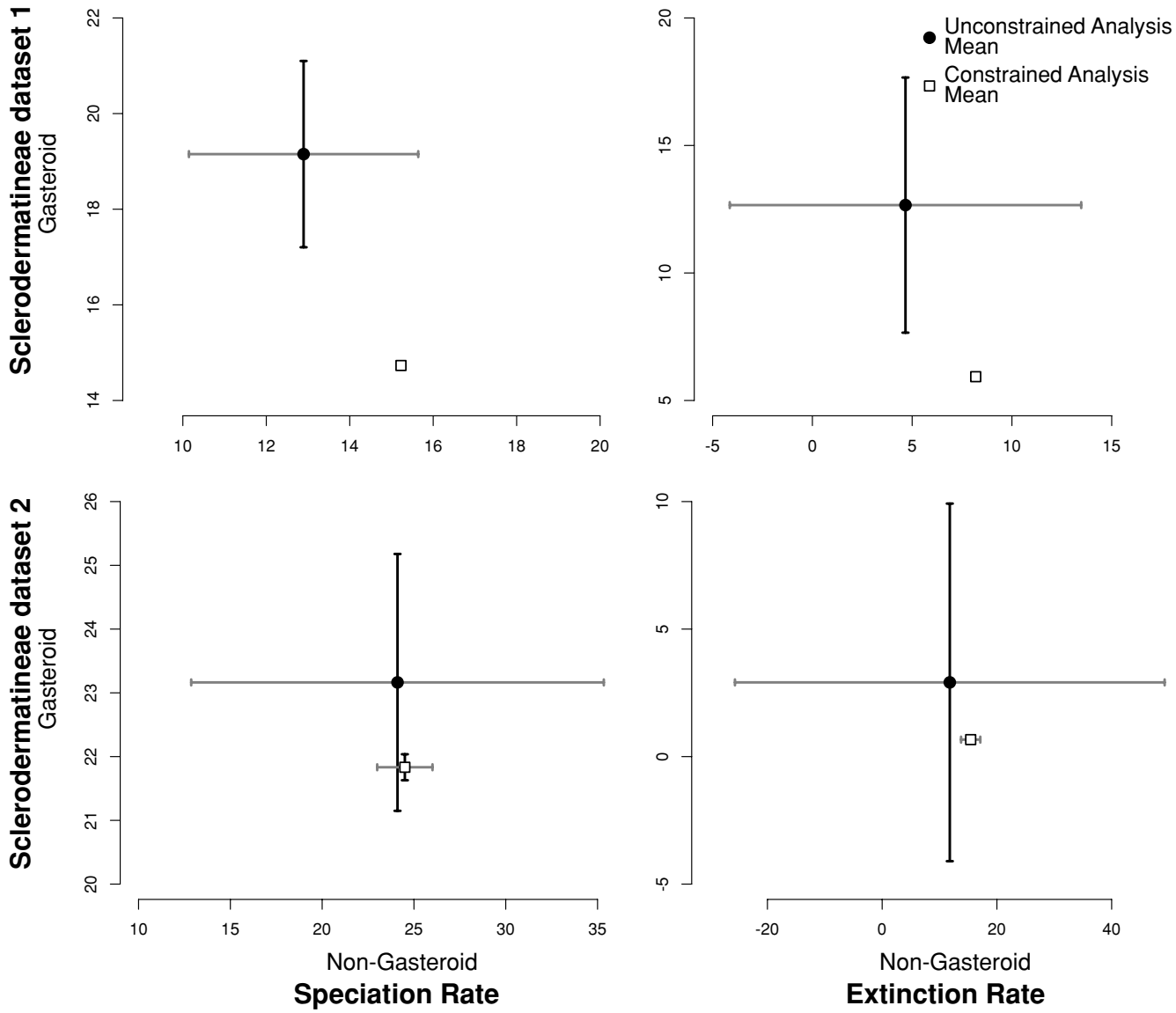

Figure 7. Means and variances for speciation and extinction rate parameters under unconstrained (without reversals; circle symbol) and constrained (with reversals; square symbol) models. Results are from 50 BiSSE maximum likelihood optimizations from Sclerodermatineae datasets 1 and 2. Variances for nongasteroid and gasteroid states indicated by gray and black bars, respectively.

diversification effects are relatively robust to modest variation in taxon sampling.

The predicted equilibrium frequencies for gasteroid forms in all four datasets are much higher than the observed 8.4% frequency of gasteroid forms across the entire Agaricomycetes. Again, one possible explanation for this discrepancy is simply that many of the gasteroid lineages outside of our focal clades are relatively young, and have not yet reached equilibrium. Indeed, many clades of gasteroid fungi are small groups that appear to be recently derived within clades of nongasteroid fungi (e.g., *Torrendia* within *Amanita*; *Thaxterogaster* within *Cortinarius* s. lat.; *Endoptychum* within *Agaricus*, etc).

Alternatively, the dynamics of diversification in the clades that we studied may not be representative of the evolutionary processes at work across the entire Agaricomycetes. Several analyses using molecular phylogenetic approaches and studies on heritability of fruiting body forms have suggested that the initial stages of the evolution of gasteroid forms may occur quickly and could have simple genetic bases (Bruns et al. 1989; Hibbett et al. 1994). The early stages of gasteromycetation are thought to involve "secotioid" forms, which have permanently enclosed spore-producing structures but in many cases have not yet lost ballistospory. Such intermediate forms have been described in multiple clades of Agaricomycetes (e.g., the secotioid form of *Lentinus tigrinus* in the Polyporales; *Gastrosuillus* in the Boletales; and *Podaxis* in the Coprinaceae). Secotioid forms, lacking both ballistospory and morphological adaptations to the gasteroid habit, could be at a selective disadvantage. The observation of a low frequency

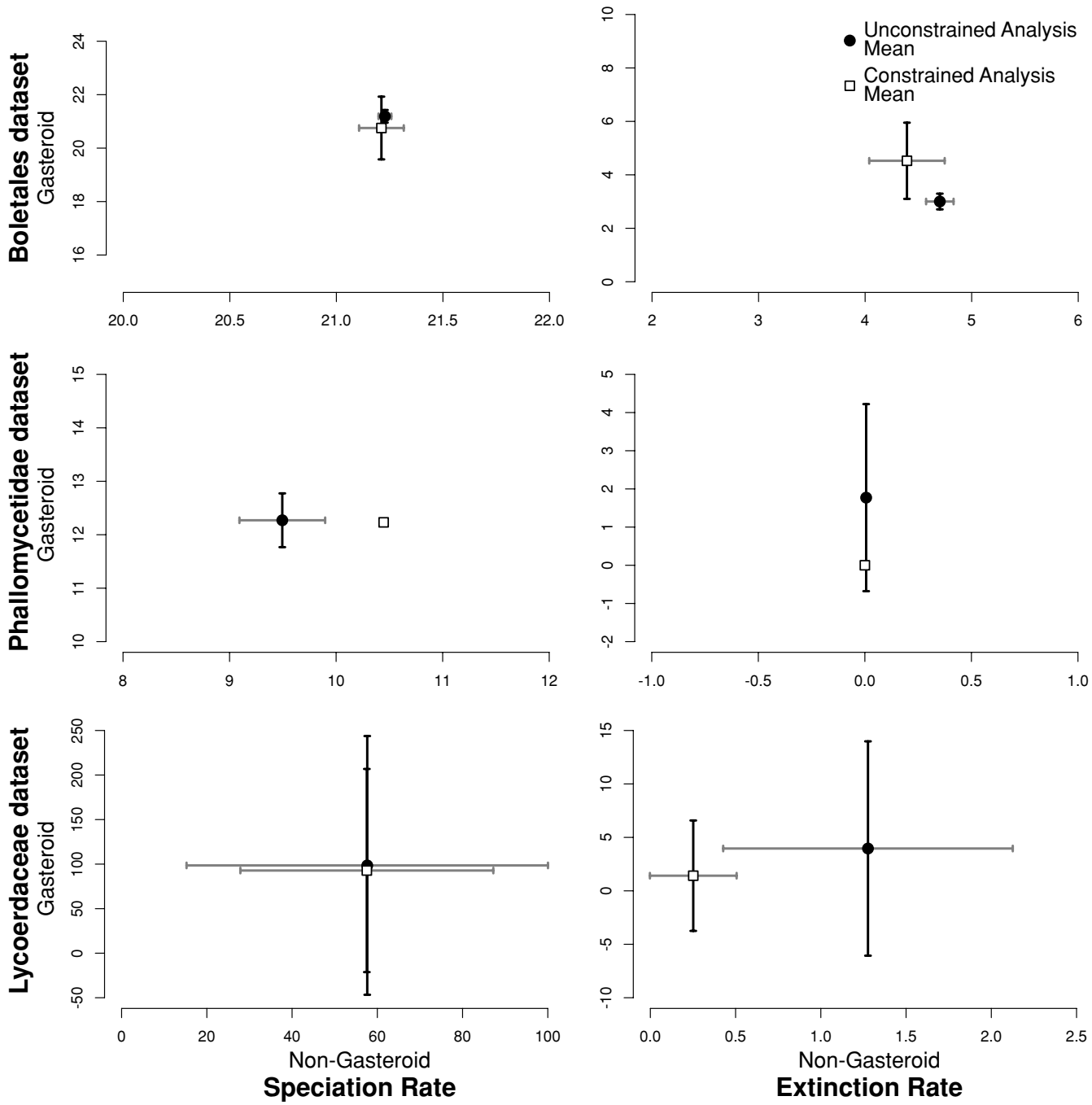

Figure 8. Means and variances for speciation and extinction rate parameters under constrained (with reversals; circle symbol) and unconstrained (without reversals; square symbol) models. Results are from 50 BiSSE maximum likelihood optimizations from Boletales, Phallomycetidae, and Lycoperdaceae datasets. Variances for nongasteroid and gasteroid states indicated by gray and black bars, respectively.

of gasteroid forms across the Agaricomycetes is consistent with the view that recently derived gasteroid forms are at high risk for extinction. The clades that we focused on in this study include highly derived gasteroid taxa, with specialized nonballistosporic spore dispersal mechanisms (Fig. 1). Indeed, the gasteromycetes studied here represent some of the most morphologically complex forms in the fungi, often with multiple functionally distinct tissues in the fruiting body and complex developmental processes. These taxa may represent exceptionally successful gasteroid lineages that have passed through the secotioid bottleneck and are now diversifying at rates comparable to, or exceeding, those of their nongasteroid relatives.

ACKNOWLEDGMENTS

We are greatly indebted to R. Fitzjohn for his patience and assistance in helping AWW implement the BiSSE analyses in Diversitree. We would like to thank R. Ree for conceptual discussions early in the development of this study, as well as constructive comments involving the review. Also, we thank T. Bruns and another anonymous reviewer for their helpful comments in reviewing this manuscript. AWW thanks S. Wagenius and D. Larkin for their assistance with programming in the R environment. We wish to thank C. Aime, R. Beever, P. Buchanan, R. Halling, K. Hosaka, T. May, G. Mueller, C. Phosri, R. Watling, and Z. Yang for specimens, sequence data and/or knowledge that contributed to this study. AWW would like to thank, Prof. Vikiniswary, A. Chan, and T. Yee Shin at the University of Malaysia, D. Desjardin from SFSU, A. Hi Harun and R. C. Ong of the FRC in Sabah for their assistance in collecting Malaysian specimens. This study was funded in part by NSF DDIG awarded to AWW (DEB-0508716) and AFTOL grants awarded to DSH (DEB-0228657 and DEB-0732968)

LITERATURE CITED

Binder, M., and A. Bresinsky. 2002. Derivation of a polymorphic lineage of Gasteromycetes from boletoid ancestors. Mycologia 94:85–98.

Binder, M., and D. S. Hibbett. 2006. Molecular systematics and biological diversification of Boletales. Mycologia 98:971–983.

Binder, M., K.-H. Larsson, B. P. Matheny, and D. S. Hibbett. 2010. Amylocorticiales ord. nov. and Jaapiales ord. nov.: early-diverging clades of Agaricomycetidae dominated by corticioid forms. Mycologia 102:865–880.

Bruns, T. D., R. Fogel, T. J. White, and J. D. Palmer. 1989. Accelerated evolution of a false-truffle from a mushroom ancestor. Nature 339:140–142.

Buller, A. 1909. Researches on fungi. Pp. 287 Longmans, Green & Co., London.

Drummond, A. J., and A. Rambaut. 2007. BEAST: Bayesian evolutionary analysis by sampling trees. BMC Evol. Biol. 7:214.

FitzJohn, R. G., W. P. Maddison, and S. P. Otto. 2009. Estimating trait-dependent speciation and extinction rates from incompletely resolved phylogenies. Syst. Biol. 58:595–611.

Gardes, M., and T. D. Bruns. 1993. ITS primers with enhanced specificity for basidiomycetes—application to the identification of mycorrhizae and rusts. Mol. Ecol. 2:113–118.

Hawksworth, D. L. 1991. The fungal dimension of biodiversity: magnitude, significance, and conservation. Mycol. Res. 95:641–655.

Hawksworth, D. L., P. M. Kirk, B. C. Sutton, and D. N. Pegler. 1996. Dictionary of the fungi. CAB International, Wallingford, UK.

Hibbett, D. S. 2004. Trends in morphological evolution in homobasidiomycetes inferred using maximum likelihood: a comparison of binary and multistate approaches. Syst. Biol. 53:889–903.

Hibbett, D. S., A. Tsuneda, and S. Murakami. 1994. The secotioid form of *Lentinus tigrinus*: genetics and development of a fungal morphological innovation. Am. J. Bot. 81:466–487.

Hibbett, D. S., E. M. Pine, E. Langer, G. Langer, and M. J. Donoghue. 1997. Evolution of gilled mushrooms and puffballs inferred from ribosomal DNA sequences. Proc. Natl. Acad. Sci. USA 94:12002–12006.

Hopple, J. S., and R. Vilgalys. 1999. Phylogenetic relationships in the mushroom genus *Coprinus* and dark-spored allies based on sequence data from the nuclear gene coding for the large ribosomal subunit RNA: divergen domains, outgroups and monophyly. Mol. Phylogenet. Evol. 13:1–19.

Hosaka, K., S. T. Bates, R. E. Beever, M. A. Castellano, W. Colgan III, L. S. Domînguez, E. R. Nouhra, J. Geml, A. J. Giachini, S. R. Kenney, et al. 2006. Molecular phylogenetics of the gomphoid-phalloid fungi with an establishment of the new subclass Phallomycetidae and two new orders. Mycologia 98:949–959.

Ingold, C. T. 1971. Fungal spores: their liberation and dispersal. Oxford Univ. Press, Oxford, UK.

Kirk, P. M., P. F. Cannon, D. W. Minter, and J. A. Stalpers. 2008. Dictionary of the Fungi. Dictionary of the Fungi, Wallingford, UK.

Læssøe, T., and L. M. Jalink. 2004. *Chlorogaster dipterocarpi*: a new peristomate gasteroid taxon of the Sclerodermataceae. Persoonia 18:421–428.

Larsson, E., and M. Jeppson. 2008. Phylogenetic relationships among species and genera of Lycoperdaceae based on ITS and LSU sequence data from north European taxa. Mycol. Res. 112:4–22.

Maddison, D. R., and W. P. Maddison. 2005. MacClade 4. Sinaur, Sunderland, MA.

Maddison, W. P., P. E. Midford, and S. P. Otto. 2007. Estimating a binary character's effect on speciation and extinction. Syst. Biol. 53:701–710.

Martín, F., J. Díez, B. Dell, and C. Delaruelle. 2002. Phylogeography of the ectomycorrhizal *Pisolithus* species as inferred from nuclear ribosomal DNA ITS sequences. New Phytol. 153:345–357.

Matheny, B. P. 2005. Improving phylogenetic inference of mushrooms with RPB1 and RPB2 nucleotide sequences (*Inocybe*; Agaricales). Mol. Phylogenet. Evol. 35:1–20.

Matheny, B. P., Y. J. Liu, J. F. Ammirati, and B. D. Hall. 2002. Using RPB1 sequences to improve phyogenetic inference among mushrooms (*Inocybe*, Agaricales). Am. J. Bot. 89:688–698.

Matheny, B. P., Z. Wang, M. Binder, J. M. Curtis, Y. W. Lim, R. H. Nilsson, K. W. Hughes, V. Hofstetter, J. F. Ammirati, C. L. Schoch, et al. 2007. Contributions of *rpb2* and *tef1* to the phylogeny of mushrooms and allies (Basidiomycota, Fungi). Mol. Phylogenet. Evol. 43:430–451.

Pagel, M. 1999. The maximum likelihood approach to reconstructing ancestral character states of discrete characters on phylogenies. Syst. Biol. 48:612–622.

Phosri, C., M. P. Martín, P. Sihanonth, A. J. S. Whalley, and R. Watling. 2007. Molecular study of the genus *Astraeus*. Mycol. Res. 111:275–286.

Pringle, A., S. N. Patek, M. Fischer, J. Stolze, and N. P. Money. 2005. The captured launch of a ballistospore. Mycologia 97:866–871.

Rehner, S. A., and E. Buckley. 2005. A *Beauveria* phylogeny inferred from nuclear ITS and EF1-α sequences: evidence for cryptic diversification and links to *Cordycepts* teleomorphs. Mycologia 97:84–98.

Savile, D. B. O. 1955. A phylogeny of the Basidiomycetes. Can. J. Bot. 33:60–104.

———. 1968. Possible interrelationships between fungal groups. Pp. 649–675 *in* G. C. Ainsworth and A. S. Sussman, eds. The fungi. An advanced treatise. Academic Press, New York.

Thiers, H. D. 1984. The secotioid syndrome. Mycologia 92:1–8.

Turner, J. C. R., and J. Webster. 1991. Mass and momentum transfer on the small scale: how do mushrooms shed their spores? Chemical Engineering Sci. 46:1145–1143.

Vilgalys, R., and M. Hester. 1990. Rapid genetic identification and mapping of enzymatically amplified ribosomal DNA from several Cryptococcus species. J. Bacteriol. 172:4238–4246.

White, T. J., T. D. Bruns, S. Lee, and J. W. Taylor. 1990. Amplification and direct sequencing of fungal ribosomal RNA genes for phyogenies. Pp. 315–322 *in* M. A. Innis, D. H. Gelfand, J. J. Sninsky, and T. J. White, eds. PCR protocols: a guide to methods and applications. Academic Press, San Diego.

Associate Editor: D. Posada

Supporting Information

The following supporting information is available for this article:

Table S1. Sequence length ranges of regions sequenced for this study.
Table S2a. Phallomycetidae dataset specimen Genbank ID numbers.
Table S2b. Lycoperdaceae dataset 25S Genbank ID numbers.
Table S2c. Boletales dataset from Binder and Hibbett (2006).
Table S3a. Taxonomic sampling of the Sclerodermatineae.
Table S3b. Taxonomic sampling of the Boletales (Binder and Hibbett 2006).
Table S3c. Taxonomic sampling of the Phallomycetidae (Hosaka, Bates et al. 2006).
Table S3d. Taxonomic sampling of the Lycoperdaceae sensu Larsson and Jeppson (2008).
Appendix S1. Testing convergence of parameters from BiSSE MCMC analyses.

Supporting Information may be found in the online version of this article.